AIAA-2002-4111

The Role of Magnetic Field Topography in Improving the Performance of High-Voltage Hall Thrusters

Richard R. Hofer and Alec D. Gallimore
University of Michigan
Ann Arbor, MI

38th AIAA/ASME/SAE/ASEE
Joint Propulsion Conference & Exhibit
7-10 July 2002
Indianapolis, Indiana

THE ROLE OF MAGNETIC FIELD TOPOGRAPHY IN IMPROVING THE PERFORMANCE OF HIGH-VOLTAGE HALL THRUSTERS

Richard R. Hofer* and Alec D. Gallimore†
Plasmadynamics and Electric Propulsion Laboratory
Department of Aerospace Engineering
University of Michigan
Ann Arbor, MI 48109 USA

Abstract

Investigations of high-voltage Hall thrusters have indicated a peak in the efficiency versus voltage characteristic that limited the maximum efficiency to specific impulses of less than 3000 s. This peak is believed to be primarily a trait of modern magnetic field design, which is optimized for discharge voltages of 300 V. The NASA-173M has been operated at 300-1000 V and 5 mg/s to investigate whether performance improvements could be realized through *in situ* variation of the magnetic field topography through the use of an auxiliary trim coil. Without the trim coil, a peak in the efficiency characteristic was observed at 600 V. The results with the trim coil energized indicate there is always some performance benefit to altering the magnetic field topography. Above 400 V, efficiencies were maintained at >50% and above 900 V, specific impulses >3000 s were demonstrated while using the trim coil. The largest gains in performance were observed at 1000 V, where the thrust, specific impulse, and efficiency improved by 10 mN, 200 s, and 5.5%, respectively, to 165 mN, 3360 s, and 51.5%. The results demonstrate that the peak in the efficiency characteristic observed without the trim coil can be mitigated when the magnetic field topography is tailored for high-voltage operation. Analysis of the magnetic field from numerical simulations has identified several important factors contributing to the performance benefits with trim coil operation.

Introduction

Mission studies have indicated that a variable specific impulse (VIPS) Hall effect thruster (HET) or ion thruster could provide substantial benefits to a variety of spacecraft missions.[1] These have included LEO and GEO stationkeeping and orbit insertion, GEO reusable tug missions, and interplanetary probes. Ironically, to achieve VIPS a need was identified with both technologies to overcome lifetime issues at specific impulses (I_{sp}) where the other technology has previously demonstrated high propellant throughput. In the case of the ion thruster, operation at I_{sp}'s as low as 1800 s was required, where grid erosion is enhanced due to decreased beamlet focusing. For the HET, operation above 3000 s was needed, where the higher energy ions are expected to cause enhanced erosion rates of chamber walls.

To address the needs identified in the mission studies, as well as on-going efforts to expand current HET technology, the NASA Glenn Research Center has in recent years initiated a multi-phased program for the development of high I_{sp} HETs.[2] In phase one, contracts were awarded to develop thrusters that demonstrate the feasibility of operating modern xenon HETs at I_{sp}'s greater than 3000 s. The three engines that were delivered were the D-80 from TsNIIMASH under contract to Boeing, the SPT-1 from Fakel under contract to the Atlantic Research Corporation, and the BHT-1000 from Busek.[3-5] The thrusters have been operated at maximum voltages and I_{sp}'s of 1700 V / 4100 s, 1250 V / 3700 s, and 1000 V / 3300 s for the D-80, SPT-1 and BHT-1000, respectively. Despite being different designs, each thruster exhibited a voltage range where the anode efficiency was maximized. This voltage was roughly between 500-800 V depending on the mass flow rate. The source of this peak efficiency was not identified, but there was speculation by some authors that the loss was being driven by increased electron current at high-voltages.[4-5]

Phase one successfully demonstrated that there were no fundamental restraints to building a HET capable of >3000 s I_{sp}. Further, despite the observed peak, anode efficiencies were still maintained above 50% for a wide range of voltages and flow rates.

* Graduate Student, Student Member AIAA, richard@hofer.com
† Associate Professor, Associate Fellow AIAA

Building on these efforts, GRC phase two objectives are to: 1) identify the physical mechanisms that result in this maximum efficiency with voltage, and 2) develop the design tools necessary to extend efficient operation beyond the 800 V ceiling recently observed. To achieve these goals, the University of Michigan has collaborated with GRC in the design and fabrication of a high- I_{sp} HET, the 5 kW NASA-173M.[6] The thruster employs a plasma lens magnetic field and a trim coil that allows for *in situ* variations of the magnetic field not possible with the common collection of inner and outer coils. While inner and outer coils alone allow for control of the magnitude of the magnetic field and some ability to alter the field line shape, the speculation when building the 173M was that, to achieve efficient operation at high-voltages, magnetic field topographies not used at lower voltages would be required. This was the primary motivation for implementing the trim coil in the 173M.

The D-80, SPT-1, and BHT-1000 all used the standard configuration of inner and outer coils; there was no reported use of trim coils. The BHT-1000 reportedly used 300 V as the design point for the thruster, with changes that allowed for higher magnetic fields to be established. Any changes to the magnetic field topography were not discussed. Whether an attempt was made to optimize the D-80 and SPT-1 field line topography for high-voltage operation was not reported, although it is reasonable to assume that the manufacturers also anticipated the requirement of higher magnetic field intensity. Apparently, changes to the D-80 and SPT-1 for high-voltage were primarily an attempt to optimize the electric field through changes to the discharge chamber. In the SPT-1, a metallic anode similar to anode layer thrusters was used for a portion of the discharge chamber with a dielectric at the exit as in conventional SPT's. In the D-80, operation as a two-stage thruster, by introducing an intermediate electrode, was employed to alter the electric field distribution.

This paper reports on the performance of the NASA-173M at voltages of 300-1000 V at a constant flow rate of 5 mg/s. At each voltage, the trim coil current was varied to determine whether efficient operation could be achieved through *in situ* control of the field line topography.

Experimental Apparatus

NASA-173M Hall Effect Thruster

The NASA-173M is a nominally 5 kW HET that may be operated as either a single- or two-stage device, and is shown in Figure 1. The thruster has an outer diameter of 173 mm, a channel width of 25 mm, and a channel depth of 38 mm. A more detailed description of the thruster and early performance measurements are given in Ref. 6. Ref. 7-8 report on plume measurements. In Ref. 6 and 7, the thruster was referred to as the P5-2. The thruster was renamed because of continuing in-house development at GRC on a second version of this thruster.

Changes to the 173M since the configuration of Ref. 6 and details of its operation for these experiments include:

1. The thruster was operated only in single-stage mode.
2. A new high-purity (>94%) boron nitride discharge chamber that uses calcium borate as a binder was fabricated without the segmented walls used for two-stage operation, as in Ref. 6. For the experiments presented here, this discharge chamber had been subjected to approximately 40 hours of operation before any measurements were taken.
3. The outer front pole was plasma sprayed with aluminum oxide.
4. The 6 mm extension to the inner wall used in Ref. 6 was replaced with a 1.5 mm boron nitride disk that was nearly flush with both the inner and outer walls.
5. A GRC laboratory model hollow cathode was located at the 12 o'clock position on the thruster. The cathode orifice was located approximately 25 mm downstream and 25 mm radially away from the outer front pole at an inclination of 30° from thruster centerline.

Plasma Lens Focusing

The NASA-173M magnetic circuit employs what is commonly referred to as a plasma lens,[9-13] established by a set of inner and outer coils and pole pieces. In a plasma lens, the field line curvature focuses ions on the channel centerline, which has been shown to extend the focal length of the plume to distances of several thruster diameters.[6] This focusing effect is possible because, at least to a first order approximation, magnetic field lines form equipotentials of the accelerating voltage.[14-15] The approximation breaks down in the presence of large electron pressure gradients.

A plasma lens affects thruster operation primarily by:

1. Increasing the magnetic insulation of the ions from the wall. This effect should be the most dramatic for ions born in weak electric fields before the ions are significantly accelerated. The field line curvature preferentially directs ions towards the channel centerline away from the walls, which

increases efficiency and lifetime while decreasing thermal loads.
2. An increase in the path length of electrons trapped on a given field line thereby increasing the ionization efficiency.
3. Focusing of the ion beam on the discharge chamber centerline. Improving the focal properties of the plume should decrease plume divergence and increase efficiency and lifetime.

Radial Trim Coil

A trim coil (TC) is generically referred to as any coil used in a HET in addition to the typical inner coil (IC) and outer coils (OC). TC's are usually used so that more control of the magnetic field topography can be obtained during thruster operation. The IC and OC generally do not allow for the types of changes that are required to modify the magnetic field over an extended operating range. A more precise method for sculpting the field would be to change the pole pieces, but this is prohibitively time-consuming and expensive from the perspective of a research program. In Ref. 13, a TC was used to identify an optimum field line topography that was later instituted in a flight version thruster through changes to the pole piece design.

TC's have been used in HETs for decades, dating back to the now seminal work by Morozov,[16] which first showed that a magnetic field that peaked at the exit was preferred for stable operation. Recently, Kim has experimented with TC's on xenon and krypton mixtures.[17] Other implementations of TC's are discussed in Ref. 13 and 18-20.

Ref. 13 discusses the use of a TC to actively change the radius of curvature of field lines, and hence the focal length, in a plasma lens. This work demonstrated that altering the focal length at low voltages could substantially increase thruster efficiency. For example, at 150 V an increase from 21% to 50% was reported. The coil was also effective at nominal operating voltages. At 350 V an increase in efficiency from 58% to 62% was observed. The maximum voltage investigated was 400 V.

The TC in the 173M is referred to as a radial trim coil because it primarily affects the radial magnetic field.[6] When the coil is energized, the radius of curvature of the plasma lens, i.e. the axial gradient of the magnetic field, can be altered. Accordingly, this changes the magnitude of the peak radial centerline field and can change both the magnitude and direction of the radial field at the anode. To a lesser extent, the axial position of the peak centerline field is also affected. The axial gradient of the radial magnetic field, $\nabla_z B_r$, can either be increased or decreased depending on the sign of the TC current. In the 173M, a negative TC current results in a radial field that subtracts from the primary field and thus increases the value of $\nabla_z B_r$. A positive TC current has the opposite effect.

Vacuum Facility

All experiments were conducted at the Plasmadynamics and Electric Propulsion Laboratory in the Large Vacuum Test Facility (LVTF). A schematic of the facility is shown in Figure 2. The LVTF is a stainless steel vacuum chamber that is 6 m in diameter and 9 m in length. The thruster was mounted at thruster station 1 as indicated in the figure and was fired away from the cryopumps. At this position, the cryopumps are approximately 2 m from the engine and the plume is allowed to freely expand approximately 7 m down the length of the chamber.

The LVTF is equipped with seven cryopumps that have a combined pumping speed of 240,000 l/s on xenon and an ultimate base pressure of 2.5×10^{-7} Torr. Chamber pressure is monitored using two hot-cathode ionization gauges mounted on the chamber walls. Pressure measurements for each gauge were corrected for xenon using the base pressure on air and a correction factor of 2.87 for xenon. The pressure in the facility at an anode and cathode flow rate of 4.98 mg/s and 0.52 mg/s, respectively, was 4.5×10^{-6} Torr when corrected for xenon. At this pressure and total flow rate, ingested neutral flow from the ambient tank environment has been previously shown to negligibly influence performance measurements in the LVTF.[21]

Power Electronics and Propellant Delivery

The plasma discharge was powered using two Sorenson DCR 600-16T supplies wired in series. In this configuration, 1200 V, 16 A power output is possible. One of the supplies was isolated from ground using Signal Transformer SU-5 isolation transformers. Using the supplies in series did not produce any noticeable change in thruster operation from previous investigations conducted on a single power supply.[6] The discharge filter consisted of a 95 μF capacitor in parallel and a 1.3 Ω resistor in series with the output of the power supplies. Other laboratory supplies were used to power the magnet coils and cathode.[6]

High-purity (99.999% pure) xenon was supplied through stainless steel feed lines with 20 and 200 sccm MKS Model 1100 Mass Flow Controllers. The controllers were calibrated after testing using a constant volume method.

Data Acquisition System

Thruster telemetry was acquired using a 22-bit Agilent Data Logger head unit (HP34970A) with a 20-channel multiplexer (HP34901A) through Agilent Benchlink software run on a Windows 98 personal computer. Voltages were read from the power supply outputs with the exception of the discharge voltage, which was monitored using a calibrated voltage divider designed for high-voltage. Currents were measured with high-accuracy shunts (i.e. low thermal drift) with the exception of the discharge current, which was measured with a Hall current probe. The entire system was calibrated before testing commenced. The estimated accuracy of the system is <1% of the reported values.

Thrust measurements were made with an inverted pendulum type thrust stand, based on the GRC design.[6] Deflection of the pendulum is monitored by recording the output voltage from an LVDT by the Agilent Data Logger. Inclination of the thruster was similarly recorded from the output voltage of an inclinometer. Corrections were later made to the data from a correlation between inclination and the LVDT. Calibrations were performed before and after thruster operation by deploying a series of known weights. A water-cooled shroud maintained at 10° C encompasses the thrust stand components to minimize thermal drift. Upon initial exposure to vacuum, the thruster was operated for at least two hours to allow for outgassing of thruster components. Thrust measurements were typically conducted at constant voltage and flow rate, in intervals of about 30 minutes, following the outgassing procedure. A calibration was always performed before and after thruster operation. To account for thermal drift, the dependence of the calibrations was linearly interpolated over time as recorded by the Agilent Data Logger.

Results

Performance measurements were collected in two sets of experiments. In the first set of experiments, the influence of the IC and OC current on performance was studied. This series was conducted over the range 300-1000 V in 100 V increments at a constant anode mass flow rate of 5 mg/s. This flow rate was chosen so that the discharge power would be 5 kW at 1000 V, the nominal power rating of the 173M, thus minimizing the risk of thermally induced failure of the thruster. Future testing is planned at higher flow rates and correspondingly higher efficiencies. The cathode was operated at 0.5 or 1.0 mg/s, which was varied to minimize thruster oscillations. No systematic dependence of cathode flow rate with the operating point was ever determined, and a majority of the data was taken at the lower flow rate. At each voltage, data was acquired by setting the IC current and varying the OC current so that different ratios of the coil current (IC/OC) could be examined. At least three values of the IC current were recorded, typically in increments of 0.5 A around a medial value that roughly minimized discharge current and oscillations, while increasing plume focusing and thrust. At each IC current, the ratio of IC/OC was varied over the range of 0.75–2.0, typically in increments of 0.2. As the experiments progressed to the 500 V series, it became evident that ratios of about 1.0 were resulting in peak performance. Subsequent data at ratios of 0.75 – 1.25 were taken at increments of about 0.1. Data above ratios of 1.25 were still taken but at increments as large as 0.5.

Thruster operation over the range of 300-800 V was stable and did not result in any particular difficulties. At 900 and 1000 V, oscillations in the discharge current were severe unless the IC and OC currents were increased to 5 A. Below 5 A, oscillations would grow until the discharge would eventually extinguish. Above 5 A, the oscillations were substantially reduced and the thruster operation behaved similar to the 300-800 V cases.

Performance data collected from this series was later analyzed to determine what coil currents resulted in the best performance. In general, the ratio of IC/OC was found to be close to unity and the particular value of the IC was found to usually increase with voltage. The relative change in the magnitude of the magnetic field is shown in Figure 3. The figure shows the normalized peak centerline value of the radial magnetic field that was computed for each operating point using a commercial 3D magnetostatic solver, Magnet 6 by Infolytica. Comparisons of the numerical simulations with fields measured with a Hall probe have on average yielded an uncertainty of no more than ±10%, which is mostly a result of inaccuracies in the probe position and orientation. In the figure, two curves are shown corresponding to operation with zero TC current and operation with the TC current corresponding to peak performance, as discussed below. All data is normalized with the field at 300 V without TC operation. The magnetic field shows a relative increase of 2.8 without TC operation, and 2.5 when the TC is used.

In the second series of experiments, the effect of the TC on thruster performance was evaluated to determine if improvements in the previous series of experiments could be realized. The thruster was operated at the same voltages and flow rates as the previous series of experiments. The IC currents from the previous study that gave the highest efficiency were used. In the case

where two IC currents yielded similar performance, the lower IC current was chosen as this would yield higher total thrust efficiency. An IC/OC current ratio of 1.0 was also used throughout. In this way, the IC and OC currents were held constant for a given voltage. A test would begin by starting at zero applied TC current and then gradually increase the current to larger negative values. Testing for a given discharge voltage was halted when it became evident that applying more negative TC current was resulting in unstable or inefficient operation. A cursory examination revealed that positive TC current always resulted in decreasing efficiency. Others have observed this trend.[13] No data is presented with positive TC current for these reasons.

The results from the TC current study are presented in Figures 4-12 and tabulated in the appendix. Discharge current, thrust, anode I_{sp}, and anode efficiency versus TC current at constant values of the IC and OC currents, discharge voltage, and flow rate are shown in each figure. When multiple data points were taken at a given TC current, only the data that resulted in the highest efficiency are presented in the figures, for the sake of clarity. Examination of the operating points with multiple sets of data (see the appendix) has on average revealed only small differences in the thrust, I_{sp}, and efficiency (typically 0.5-1 mN, 10-20 s, and 0.1-0.5%). This demonstrates the repeatability of the data and establishes an estimate of the relative error between data points (discussed later).

At 800 V, in addition to testing the optimum coil currents determined from the first series of experiments, the IC and OC currents were increased by 1.0 A. Figures 9 and 10 show 800 V data at 3.5 and 4.5 A on the coils, respectively. The data for 800 V and 4.5 A on the coils shows an additional 0.5% improvement in the efficiency over the 3.5 A case. Unfortunately, during testing this method of increasing the coil currents was not systematically investigated at other voltages.

Figure 13 plots the TC current that resulted in the peak efficiency at each discharge voltage. Two data points are shown for 800 V, corresponding to 3.5 or 4.5 A on the IC and OC. Note the large change in the required TC current as the IC and OC currents are increased from 3.5 to 4.5 A.

Figures 14-17 present discharge current, thrust, anode I_{sp}, and anode efficiency, respectively, versus discharge voltage. In each figure, two curves are shown corresponding to operation with zero TC current and operation with the TC currents shown in Figure 13. Note that the TC always resulted in some improvement in thruster performance over the entire voltage range.

Concerning the uncertainty in the measurements, it should be noted that while the absolute error of any experimental value can be large, the relative error between data points can be much less depending on how the data is collected. Recall that thrust data with the TC was taken at constant values of the voltage and mass flow rate. Uncertainty in the thrust, mass flow rate, current, and voltage would therefore be a constant offset to the data. An error analysis estimated the average relative error at a given voltage to be 0.7 mN, 15 s, and 0.3%, for the thrust, I_{sp}, and efficiency, respectively. The error between data at different voltages would be quantified more by the absolute error, which is dominated by the uncertainty in the thrust and anode flow controller. Analysis has shown the average uncertainty for both the thrust and anode flow controller to be ±1.5% of the measured value. Since the efficiency increase with TC operation were on average 2% (a maximum of 5.5% was observed at 1000 V), it was concluded that the trends shown in the figures are not a result of relative measurement error. The average improvement for the I_{sp} and thrust was 70 s and 3 mN, respectively, which were also greater than the relative error estimates. The maximum improvement in the I_{sp} and thrust was 200 s and 10 mN, respectively, both of which occurred at 1000 V.

Lastly, an extensive series of numerical simulations using Magnet was conducted at each of the coil currents found through the experiments, both with and without TC operation. Figure 18 shows the field line topography for a series of test cases corresponding to 1000 V operation. Specifically, the IC and OC currents are each set to 5 A and the TC current is set to 0, -1, -2, and -3 A. The 0 A TC case is representative of the field lines at other voltages where the TC was not used. In general, at voltages of 300-700 V, the optimum TC current was lower than the 1000 V case. So for these voltages, the increase in the field line curvature more closely resembled the -1 A case in Figure 18, or less depending on the particular TC current. At 800-1000 V, -2 A TC current is the optimum determined in the experiments, but note that 800 V optimized at the slightly lower value of 4.5 A for the IC and OC.

Discussion

The first series of experiments revealed that a ratio near 1.0 for the IC/OC current resulted in peak performance. In Ref. 6, ratios of 1.2-1.6 were determined to be optimum, but that series of experiments unfortunately did not consider ratios of 1.0. Numerical simulations with Magnet have shown that a symmetric plasma lens is realized for coil current ratios near 1.5, so it is surprising to find better performance at ratios of 1.0. A likely explanation is the result of the higher outer wall

magnetic fields that result at low IC/OC current ratios. The plasma location is governed by a balance between the pressure and the magnetic field, as illustrated by the single-fluid MHD approximation,

$$\frac{\partial}{\partial r}\left(P + \frac{B^2}{2\mu_0}\right) = 0 \qquad (1)$$

Thus, creating a minimum in the radial magnetic field profile across the channel tends to locate the plasma on centerline. At IC/OC ratios of 1.5, the peak outer wall to centerline magnetic field ratio is 1.13 and increases to 1.22 for IC/OC ratios of 1.0. This may indicate a need to modify the fixed magnetic structure of the 173M so that higher outer wall fields are possible for symmetric field line topographies. In general, the performance would begin to decrease at IC/OC ratios less than unity. This is attributed to shifting the plasma lens symmetry far enough off centerline that other inefficiencies resulting from the asymmetry begin to dominate. For example, changes in the magnetic field could alter the distribution and location of the Hall current, which would impact the ionization and acceleration efficiency, as well as the stability, of the thruster. Ref. 12 discusses the necessity of symmetry in a plasma lens. In those experiments, when the lens was shifted off chamber centerline, an increase in discharge current and plume divergence was observed. Figure 18 also supports these conclusions. At 1000 V, as the TC grew more negative, the field line topography gradually became more symmetric about the channel centerline. The numerical simulations also show that the ratio of the outer wall to centerline field remained relatively constant with TC current. However, it was not concluded that the performance benefits of the TC were a result solely of the lens being restored to a symmetric field. In fact, most of the TC currents at voltages of 300-600 V only marginally shifted the lens back to centerline. Other contributing factors to the performance benefit of the TC are discussed later.

There is some disagreement in the literature concerning the scaling of the magnetic field with voltage. The long held belief is that the magnetic field is proportional to the square root of the voltage ($B \sim V^{1/2}$).[9] Scaling employed by others suggests that the dependence is linear ($B \sim V$).[5,22] A power law curve fit to the data in Figure 3 yields an exponent of 1.5 with no TC current, and 1.2 when the TC is applied. Both fits are greater than the theoretical scaling relationships. This may be a consequence of the practical reality of building a HET that operates over a large voltage range. It is unlikely, even with the TC, that thruster performance is truly optimized at every voltage that was investigated. It seems more likely that a similarly sized thruster built for and operated at a specific voltage would perform better than the 173M for the same flow rate. In such a thruster, the magnetic field intensity should more closely obey theoretical scaling relationships. A high-voltage, single set point HET may not be of much interest, however, especially in light of mission studies requiring VIPS operation.

Numerical simulations of a 50 W anode layer thruster at 300-1200 V showed that the peak in the efficiency curve (600 V) could be avoided if the magnetic field intensity was sufficiently large.[23] In the simulations, the magnetic field was scaled to higher values relative to the field at 300 V, i.e. there were no changes to the field line topography. At 1200 V, the required field intensity was twice that at 300 V. The magnetic field was also found to scale linearly with voltage. For the 173M at 1000 V, Figure 3 shows a relative increase of 2.8 without TC operation, and 2.5 when the TC is used. Note that experiments without the TC were performed in the same manner as Ref. 23, i.e. the field line topography was constant, only the relative intensity increased. The results of these experiments indicate that merely increasing the magnetic field intensity is not sufficient to maintain a monotonically increasing efficiency with voltage. Changes to the magnetic field topography, as evidenced by the TC data, support this conclusion. These results contradict the findings of Ref. 23. The 173M experiments are also supported by the previously discussed performance evaluations of the D-80, SPT-1, and BHT-1000. Differences in the performance trends between experiment and simulation may also be a result of thruster design limitations. In a numerical simulation, there are no thermal limits or other practical realities that must be addressed in thruster design. In this light, the simulations are encouraging, as they imply that further improvements may be possible. For a VIPS thruster, however, the 173M experiments have shown that variable field line topography will most likely be required.

The variation of performance with TC current presented in Figures 4-12 displays a remarkable level of complexity. In the ensuing discussion, only the most general trends are commented on, as a discussion of each voltage is not warranted. First, consider the 300 V data of Figure 4. As the TC current is increased (more negative) an increase in thrust is accompanied by a decrease in the discharge current. The result is an increase in the I_{sp} and efficiency. At some point, maximum thrust is reached but the current continues to fall. Since efficiency scales with the thrust squared, the ensuing drop in thrust causes the I_{sp} and efficiency to fall as well. A minimum in the discharge current is later shown, and the performance correspondingly

continues to plummet when the current later increases past the minimum.

Considering the data as a whole, many of the trends shown at 300 V are repeated. The general trend in the thrust is to initially increase, reach a maximum, and then continually fall. Some notable exceptions are 600 V, 800 V (3.5 A), and 900 V. At 600 V, a small decrease is initially shown, after which a maximum is found. At 800 V (3.5 A) and 900 V, the thrust is still increasing at the last TC data point but the efficiency is falling. The general trend for the discharge current is to either initially decrease with TC current or remain approximately constant. Only the 400 V case continually increased with TC current. There was usually a critical TC current after which the discharge current would quickly increase. This is likely attributed to an increase in the field line curvature such that a portion of the electrons in the discharge chamber are shorted to the anode, increasing the axial electron current. The field lines in Figure 14 support this conclusion as well.

Because the discharge current is the sum of the ion and electron currents, simply knowing the relative change in discharge current is not always sufficient to determine whether it is the ions or electrons that are being affected the most. Following the trends in the thrust and the efficiency aids in this determination, but there are still inconclusive cases. Measurements of the plasma parameters inside the discharge chamber and a measurement of the ion current (and hence, electron current) at or near the exit plane are needed to better understand these trends.

The results at 800 V shown in Figures 9 and 10 suggest that further improvements in the efficiency may be achieved at other voltages. In Figure 9, the IC and OC currents were 3.5 A, and in Figure 10 these were set to 4.5 A. The 3.5 A case demonstrates the highest efficiency without the TC, but a lower peak efficiency than at 4.5 A. This is probably due to the relative reduction in the magnetic field from using the TC. Using higher IC and OC currents with the TC maintains the magnetic field at the levels encountered at the lower IC and OC currents without the TC. Taken together, Figures 9 and 10 highlight the importance of both the magnitude and shape of the magnetic field in achieving peak performance.

The composite data comparing operation with and without the TC in Figures 14-17 show some important trends. In Figure 14, the discharge current rises by more than 1 A as the voltage is increased. Use of the TC tended to lower the current at each voltage, but the current still increased overall with increasing voltage. Increased electron current or greater fractions of multiply-charged species are possible explanations of these trends. Measurements of ion current and the ion species fractions are needed, however, to reach further conclusions. In Figure 15, an increase in thrust is always observed with the TC, resulting in a corresponding increase in the I_{sp} as shown in Figure 16. Above 900 V, specific impulses >3000 s were demonstrated with the TC. The trend that the thrust increased while the discharge current decreased with TC operation, is an important result. This implies that the TC is either increasing the mass utilization and/or increasing the focusing of the ion stream while simultaneously decreasing the electron current. It is most likely a combination of all the above and voltage dependent. This further motivates the need for probe measurements.

The trends in the discharge current and thrust are brought together in the efficiency characteristic shown in Figure 17. Without the TC, the efficiency is shown to peak at 600 V and then continually decrease. This is the same behavior that was observed in the D-80, SPT-1, and BHT-1000. The results with the TC indicate there is always some performance benefit to altering the magnetic field topography. Above 400 V, efficiencies were maintained at >50% while using the TC. Beyond 600 V, operation with the TC initially decreases but reaches another minimum at 800 V, after which the efficiency increases at 900 and 1000 V. The largest gains in performance were observed at 1000 V, where the thrust, specific impulse, and efficiency improved by 10 mN, 200 s, and 5.5%, respectively, to 164.9 mN, 3362 s, and 51.5%. Overall, the performance trends demonstrate that the peak in the efficiency characteristic observed without the TC can be mitigated when the magnetic field topography is tailored for high-voltage operation.

In an attempt to quantify what changes in the magnetic field topography were influencing the performance trends the most, the results from the numerical simulations of the magnetic field were analyzed. Several important characteristics believed to be important in a plasma lens were investigated. The results of this analysis indicated that the two most important factors, other than field line shape, characterizing the changes in the field were the magnitude of the magnetic field at the anode and the variation of the axial gradient of the radial magnetic field.

A magnetic field near zero at the anode is desirable because this lowers the fall voltage in the anode sheath. Radial magnetic fields across the face of the anode decrease the axial mobility of electrons resulting in a

fall voltage to maintain current continuity. It is undesirable for electric fields to persist deep in the channel as this increases the likelihood of ions being accelerated into the channel walls. While avoiding anode falls should improve performance, this does not explain the performance benefits observed at 800 V (4.5 A) and above. At those voltages, because the TC current was so large, the radial magnetic field actually reverses direction and grows in magnitude. The magnitude of the radial magnetic field at the anode on centerline ($|B_{r,anode}|$) is about 14% of the maximum radial field on centerline ($B_{r,max}$). In comparison, without the TC $|B_{r,anode}|$ is about 6% of $B_{r,max}$, and for voltages of 800 V (3.5 A) or less, this is reduced to 2%. The tendency then was for the TC to drive the anode field towards zero except for the data that utilized the most negative values of the TC current. In conclusion, it does not seem that the anode field is the only factor behind the measured benefits to thruster performance.

In the past, researchers have found that the axial gradient of the radial magnetic field strongly influences performance.[9-10,24] Their approach was to define an average value of the gradient based off the inverse of the scale length of variation of the radial magnetic field. It appears that this length scale, L_B, was defined either as the distance from the anode to $B_{r,max}$, or as the distance from $B_{r,max}$ to the position where the field falls to $0.80*B_{r,max}$. Because this approach has units of inverse length (L^{-1}), it may not be applicable to thrusters with different channel lengths. When applied to the fields encountered in the 173M, there was no strong correlation between either of these definitions of L_B and the operating point. As a result, it was concluded that a non-dimensional axial gradient might be more applicable. To define this number, the average gradient of the centerline radial magnetic field is defined as,

$$\left\langle \nabla_z B_r \right\rangle \equiv \frac{B_{r,\max} - B_{r,anode}}{z_{\max} - z_{anode}} \qquad (2)$$

where z_{max} is the axial coordinate of $B_{r,max}$, and z_{anode} is the axial coordinate of the anode. To non-dimensionalize the average gradient, a characteristic length scale and magnetic field are needed. $B_{r,max}$ was chosen for the magnetic field and the scale length is chosen as the distance from $B_{r,max}$ to the anode,

$$L_B \equiv z_{\max} - z_{anode} \qquad (3)$$

With these choices, the non-dimensional average gradient of the centerline radial magnetic field is defined as,

$$\zeta \equiv \frac{L_B}{B_{r,\max}} \times \left\langle \nabla_z B_r \right\rangle = \frac{B_{r,\max} - B_{r,anode}}{B_{r,\max}} \qquad (4)$$

The definition of ζ, while arbitrary, removes the dependence of the channel in the calculation. This seems appropriate because HET's are, in general, designed with $B_{r,max}$ located at or near the exit plane.[9] Thus, for a given channel length, the value of ζ yields additional information about $B_{r,anode}$. When the value of ζ is equal to unity, $B_{r,anode}$ is exactly zero. Values less than one imply a positive value of $B_{r,anode}$ and values greater than one imply a negative value of $B_{r,anode}$. Figure 19 plots the value of ζ for each voltage in these experiments. Without the TC, ζ is a constant value of 0.94. For moderate values of the TC current (300-800 V [3.5 A]), the value of ζ is on average 1.00. When the TC current is large (800 [4.5 A]-1000 V), the value of ζ noticeably increases to an average value of 1.14. The implication of Figure 19 is that high-voltage thrusters may benefit from short channel lengths and steep gradients in the magnetic field. Accordingly, the performance of the 173M at voltages above 800 V may see further improvements if the anode is repositioned to the point where the centerline radial field vanishes. This point closely corresponds to the saddle point shown in the field lines of Figure 18. Similar improvements may also be found at lower voltages. Studies of channel length dependence have been hindered in the past because they usually did not change the magnetic field gradient along the length of the channel or the gas distributor.[25-26] So long as the magnetic field is properly modified, the real challenge of a short channel is maintaining uniform flow distribution. Apparently, these difficulties have been largely overcome in the BPT-4000, which employs a channel width to length ratio of 2:1.[13] A long, narrow anode may also be a viable solution. Such a configuration would closely resemble the anode in the D-80.[3]

Conclusions

These experiments have documented a series of investigations of the influence of magnetic field topography on Hall thruster performance. The peak in the efficiency characteristic also found in a variety of other thrusters has been largely attributed to the inadequacy of simply scaling the magnetic field intensity with voltage for a fixed magnetic structure. For the experiments presented here, when the field line topography was altered with a trim coil, the peak in the efficiency curve was mitigated at higher voltages. Analysis of the magnetic field from numerical simulations has identified several factors contributing to

the performance benefits shown with trim coil operation. These factors are:

1) The overall symmetry and radius of curvature of the field line topography,
2) The magnitude and direction of the radial magnetic field at the anode face,
3) The axial gradient of the centerline radial magnetic field, which has been characterized by a non-dimensional parameter.

Other factors that have been found to be common to high-voltage operation either with or without the trim coil are:

1) The ratio of the radial field at the walls compared to the centerline value,
2) The magnitude of the magnetic field.

Future Work

The trends observed in the performance with changing trim coil current have demonstrated a need for a rigorous examination of high-voltage Hall thrusters through probe-based diagnostics. Specifically, the following measurements, as a function of voltage and magnetic field topography are needed:

1. Exit-plane ion current density measurements using a Faraday cup to determine the ion and electron current,
2. Species fractions for multiply-charged xenon ions using an ExB probe or time-of-flight mass spectrometer,
3. Measurements of the number density, electron temperature, and plasma potential inside the discharge chamber.

In the near future, ion current density measurements will first be considered. Operation at higher flow rates (and hence, higher efficiencies) will also be investigated. Modifications to the fixed magnetic structure in the 173M are also under consideration, as well as the anode and channel length configurations suggested by the magnetic field analysis.

Acknowledgements

The authors would like to acknowledge the support of this research by the NASA Glenn Research Center through contract NGT3-52349 and NAG3-2307 (Robert Jankovsky, technical monitor for both grants).

References

1. Oleson, S. R., "**Mission Advantages of Constant Power, Variable I_{sp} Electrostatic Thrusters**," AIAA-2000-3413, 36th Joint Propulsion Conference, Huntsville, AL, July 17-19, 2000.
2. Jankovsky, R. S, Jacobson, D. T., Sarmiento, C. J., Pinero, L. R., Manzella, D. H., Hofer, R. R., Peterson, P. Y., "**NASA's Hall Thruster Program 2002**," AIAA-2002-3675, 38th Joint Propulsion Conference, Indianapolis, IN, July 7-10, 2002.
3. Jacobson, D. T., Jankovsky, R. S., Rawlin, V. K., Manzella, D. H., "**High Voltage TAL Performance**," AIAA-2001-3777, 37th Joint Propulsion Conference, Salt Lake City, UT, July 8-11, 2001.
4. Manzella, D. H., Jacobson, D. T., Jankovsky, R. S., "**High Voltage SPT Performance**," AIAA-2001-3774, 37th Joint Propulsion Conference, Salt Lake City, UT, July 8-11, 2001.
5. Pote, B., Tedrake, R., "**Performance of a High Specific Impulse Hall Thruster**," IEPC-01-035, 27th International Electric Propulsion Conference, Pasadena, CA, Oct 14-19, 2001.
6. Hofer, R. R., Peterson, P. Y., Gallimore, A. D., "**A High Specific Impulse Two-Stage Hall Thruster with Plasma Lens Focusing**," IEPC-01-036, 27th International Electric Propulsion Conference, Pasadena, CA, Oct 14-19, 2001.
7. Hofer, R. R, Walker, M. L., Gallimore, A. D., "**A Comparison of Nude and Collimated Faraday Probes for Use with Hall Thrusters**," IEPC-01-020, 27th International Electric Propulsion Conference, Pasadena, CA, Oct 14-19, 2001.
8. Walker, M. L., Hofer, R. R., Gallimore, A. D., "**The Effects of Nude Faraday Probe Design and Vacuum Facility Backpressure on the Measured Ion Current Density Profile of Hall Thruster Plumes**," AIAA-2002-4253, 38th Joint Propulsion Conference, Indianapolis, IN, July 7-10, 2002.
9. Kim, V., "**Main Physical Features and Processes Determining the Performance of Stationary Plasma Thrusters**," Journal of Propulsion and Power, Vol. 14, No. 5, Sept-Oct, 1998, pp. 736-743.
10. Gavryshin, V. M., Kim, V., Kozlov, V. I., Maslennikov, N. A., "**Physical and Technical Bases of the Modern SPT Development**," 24th International Electric Propulsion Conference, Moscow, Russia, Sept 19-23, 1995.
11. Valentian, D., Bugrova, A., Morozov, A., "**Development Status of the SPT MK II Thruster**," IEPC-93-223, 23rd International Electric Propulsion Conference, Seattle, WA, Sept 13-16, 1993.

12. Belikov, M. B., Gorshkov, O. A., Rizakhanov, R. N., Shagayda, A. A., "**Hall-Type Low- and Mean-Power Thrusters Output Parameters**," AIAA-99-2571, 35th Joint Propulsion Conference, Los Angeles, CA, June 20-24, 1999.
13. King, D. Q., de Grys, K. H., Jankovsky, R., "**Multi-Mode Hall Thruster Development**," AIAA-2001-3778, 37th Joint Propulsion Conference, Salt Lake City, UT, July 8-11, 2001.
14. Morozov, A. I., "**Focusing of Cold Quasineutral Beams in Electromagnetic Fields**," Soviet Physics – Doklady, Vol. 10, No. 8, Feb., 1966.
15. Bugrova, A. I., Morozov, A. I., Popkov, G. B., Kharchevnikov, V. K., "**Characteristics of a Plasma Lens**," Soviet Physics – Technical Physics, Vol. 31, No. 2, Feb., 1986.
16. Morozov, A. I., Esipchuk, Y. V., Kapulkin, A. M., Nevrovskii, V. A., Smirnov, V. A., "**Effect of the Magnetic Field on a Closed-Electron-Drift Accelerator**," Soviet Physics – Technical Physics, Vol. 17, No. 3, pp. 482-487, Sept, 1972.
17. Kim, V., Popov, G., Kozlov, V., Skrylnikov, A., Grdlichko, D., "**Investigation of SPT Performance and Particularities of its Operation with Kr and Kr/Xe Mixtures**," IEPC-01-65, 27th International Electric Propulsion Conference, Pasadena, CA, Oct 14-19, 2001.
18. Morozov, A. I., Esipchuk, Y. V, Tilinin, G. N., Trofimov, A. V., Sharov, Y. A., Shchepkin, G. Y., "**Plasma Accelerator with Closed Electron Drift and Extended Acceleration Zone**," Soviet Physics – Technical Physics, Vol. 17, No. 1, pp. 38-45, July, 1972.
19. Bugeat, J. P., Koppel, C., "**Development of a Second Generation of SPT**," IEPC-95-35, 24th International Electric Propulsion Conference, Moscow, Russia, Sept 19-23, 1995.
20. Kim, V., Grdlichko, D., Kozlov, V., Lazurenko, A., Popov, G., Skrylnikov, A., Day, M., "**SPT-115 Development and Characterization**," AIAA-99-2568, 35th Joint Propulsion Conference, Los Angeles, CA, June 20-24, 1999.
21. Hofer, R. R., Peterson, P. Y., Gallimore, A. D., "**Characterizing Vacuum Facility Backpressure Effects on the Performance of a Hall Thruster**," IEPC-01-045, 27th International Electric Propulsion Conference, Pasadena, CA, Oct 14-19, 2001.
22. Khayms, V., Martinez-Sanchez, M., "**Design of a Miniaturized Hall Thruster for Microsatellites**," AIAA-96-3291, 32nd Joint Propulsion Conference, Lake Buena Vista, FL, July 1-3, 1996.
23. Blateau, V., Martinez-Sanchez, M., Batishchev, O., Szabo, J., "**PIC Simulation of High Specific Impulse Hall Effect Thruster**," IEPC-01-37, 27th International Electric Propulsion Conference, Pasadena, CA, Oct 14-19, 2001.
24. Gavryushin, V. M., Kim, V. P., Kozlov, V. I., Kozubsky, K. N., Popov, G. A., Sorokin, A. V., Day, M. L., Randolph, T., "**Study of the Effect of Magnetic Field Variation, Channel Geometry Change and Its Walls Contamination Upon the SPT Performance**," AIAA-94-2858, 30th Joint Propulsion Conference, Indianapolis, IN, June 27-29, 1994.
25. Mikami, K., Komurasaki, K., Fujiwara, T., "**Optimization of Channel Configuration of Hall Thrusters**," IEPC-95-33, 24th International Electric Propulsion Conference, Moscow, Russia, Sept 19-23, 1995.
26. Cohen-Zur, A., Fruchtman, A., Ashkenazy, J., Gany, A., "**Channel Length and Wall Recombination Effects in the Hall Thruster**," AIAA-2000-3654, 36th Joint Propulsion Conference, Huntsville, AL, July 17-19, 2000.

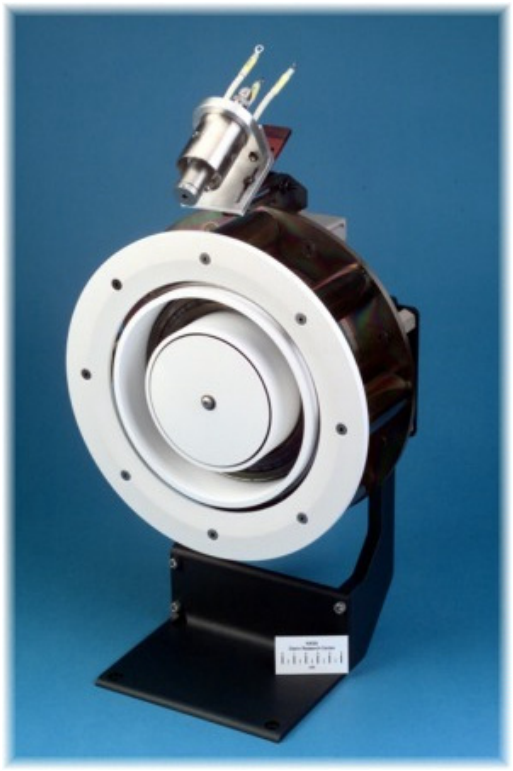

Figure 1 - Photograph of the NASA-173M.

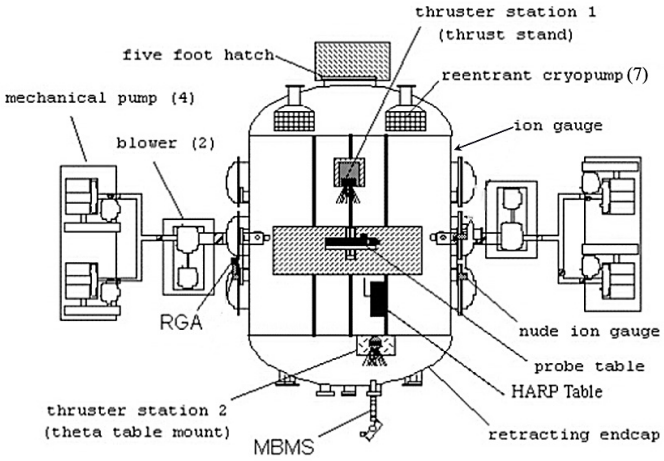

Figure 2 - Schematic of the LVTF.

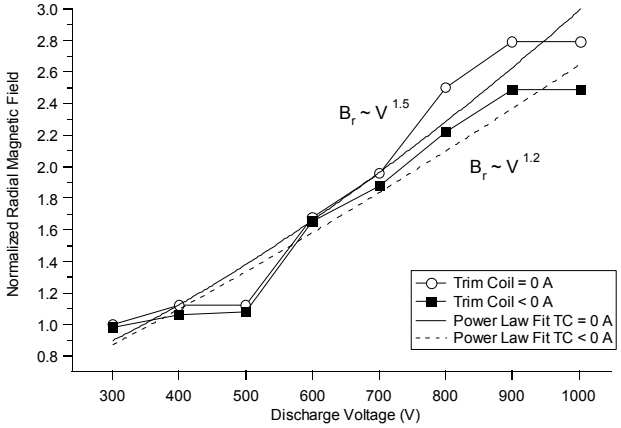

Figure 3 - Variation of the peak radial magnetic field on channel centerline vs. discharge voltage. Both data sets are normalized to the radial field at 300 V with 0 A on the trim coil. Power law curve fits showing the scaling of the magnetic field with voltage are shown.

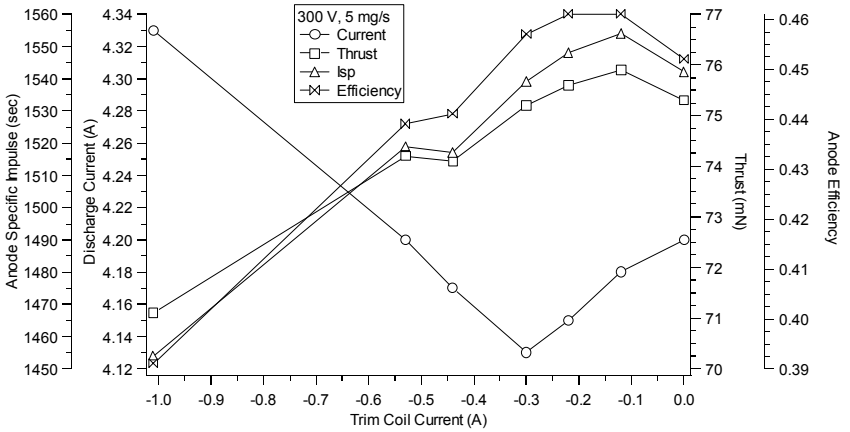

Figure 4 - Performance vs. trim coil current at 300 V, 5 mg/s.

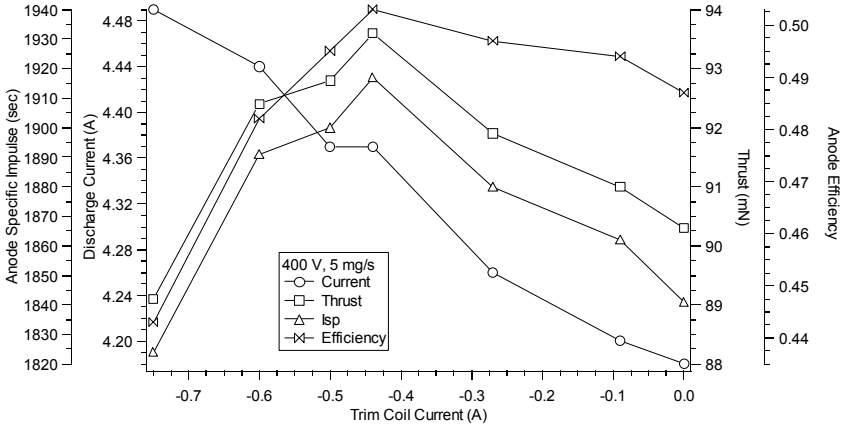

Figure 5 - Performance vs. trim coil current at 400 V, 5 mg/s.

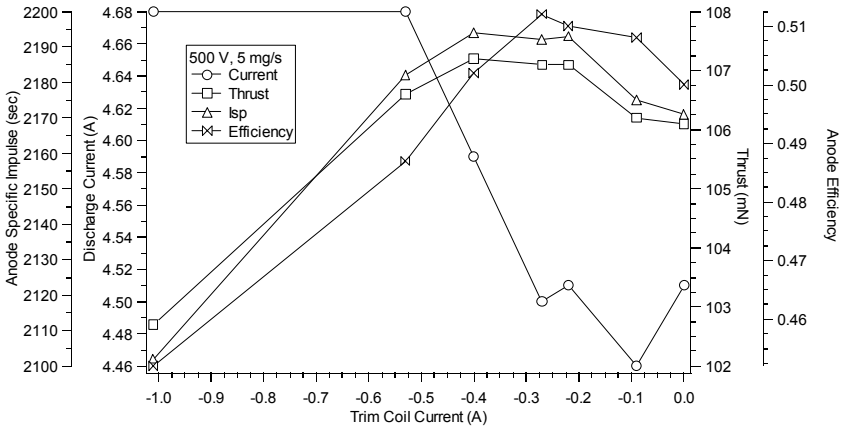

Figure 6 - Performance vs. trim coil current at 500 V, 5 mg/s.

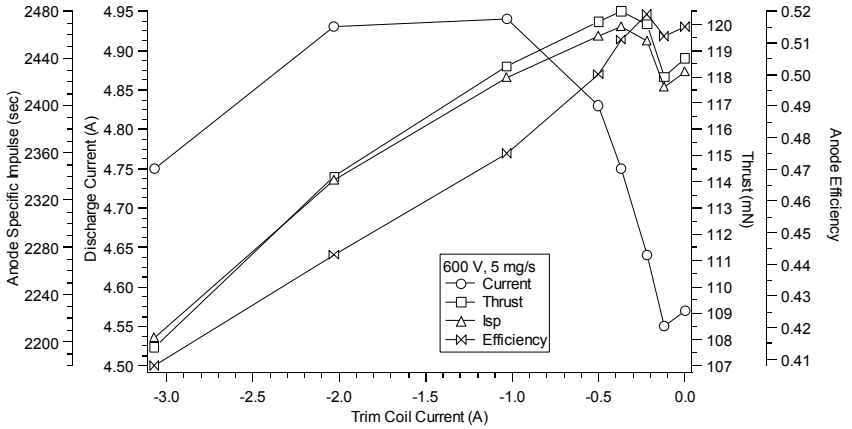

Figure 7 - Performance vs. trim coil current at 600 V, 5 mg/s.

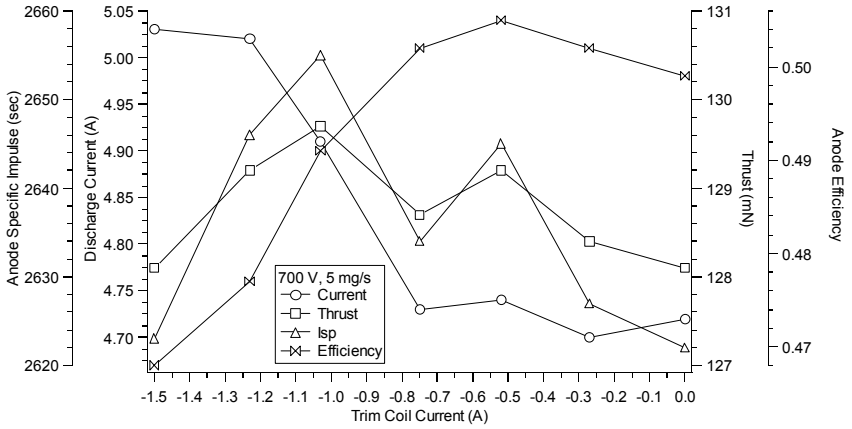

Figure 8 - Performance vs. trim coil current at 700 V, 5 mg/s.

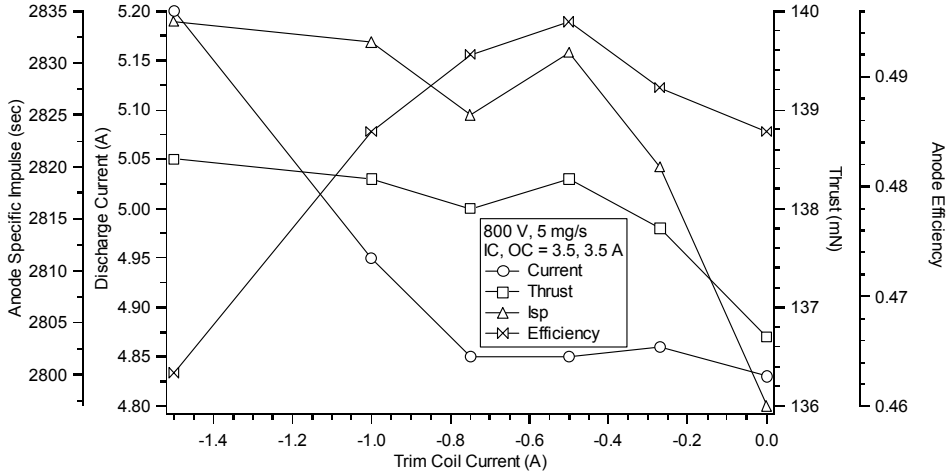

Figure 9 - Performance vs. trim coil current at 800 V, 5 mg/s with the inner and outer coils at 3.5 A.

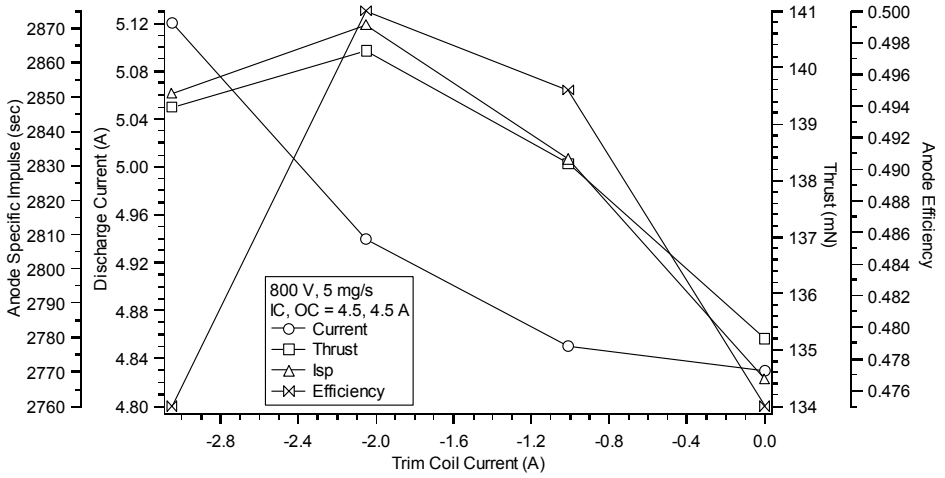

Figure 10 - Performance vs. trim coil current at 800 V, 5 mg/s with the inner and outer coils at 4.5 A.

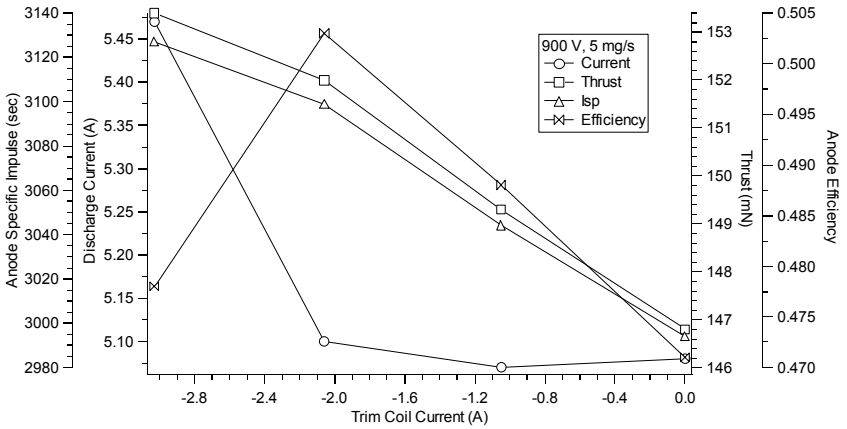

Figure 11 - Performance vs. trim coil current at 900 V, 5 mg/s.

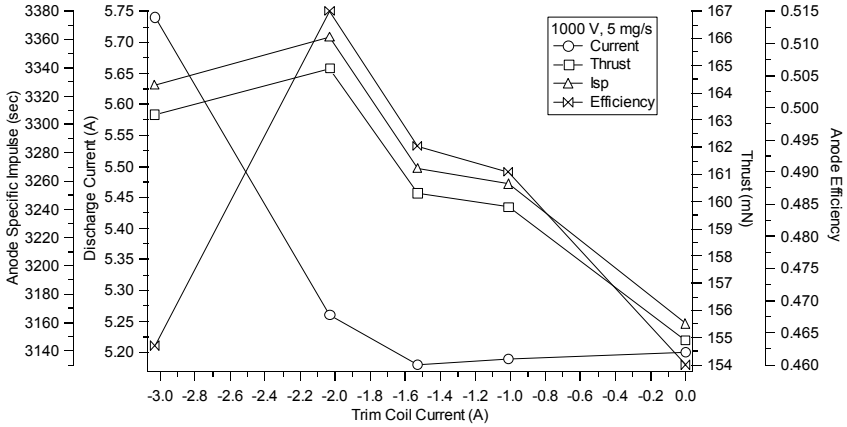

Figure 12 - Performance vs. trim coil current at 1000 V, 5 mg/s.

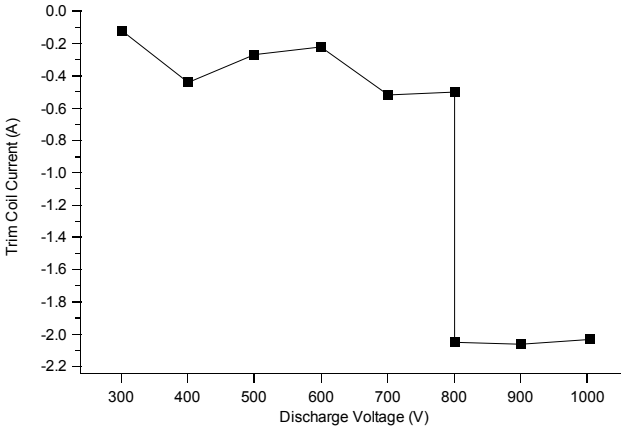

Figure 13 - Trim coil current versus discharge voltage at 5 mg/s.

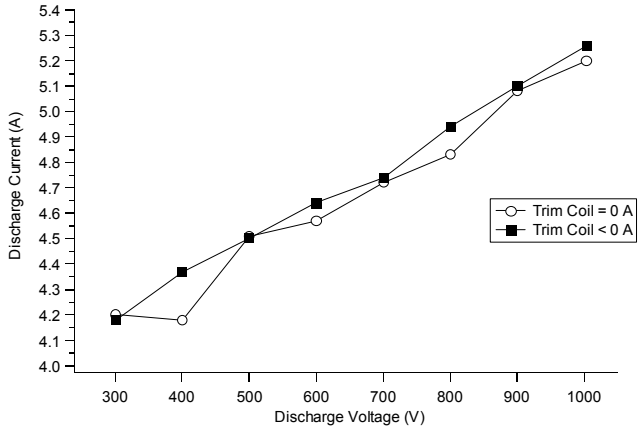

Figure 14 - Discharge current vs. voltage for operation with and without the trim coil at 5 mg/s.

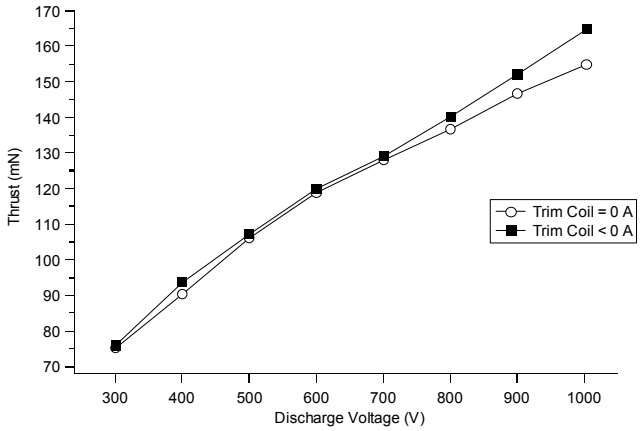

Figure 15 - Thrust vs. discharge voltage for operation with and without the trim coil at 5 mg/s.

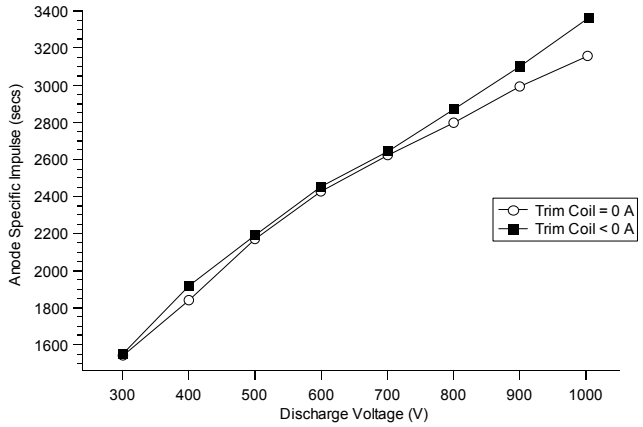

Figure 16 - Anode specific impulse vs. discharge voltage for operation with and without the trim coil at 5 mg/s.

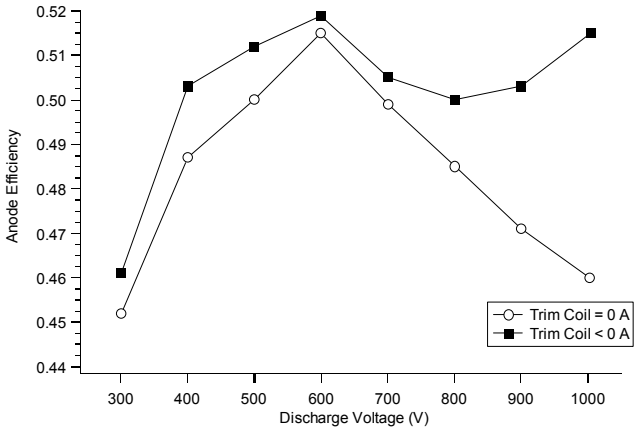

Figure 17 - Anode efficiency versus discharge voltage for operation with and without the trim coil at 5 mg/s.

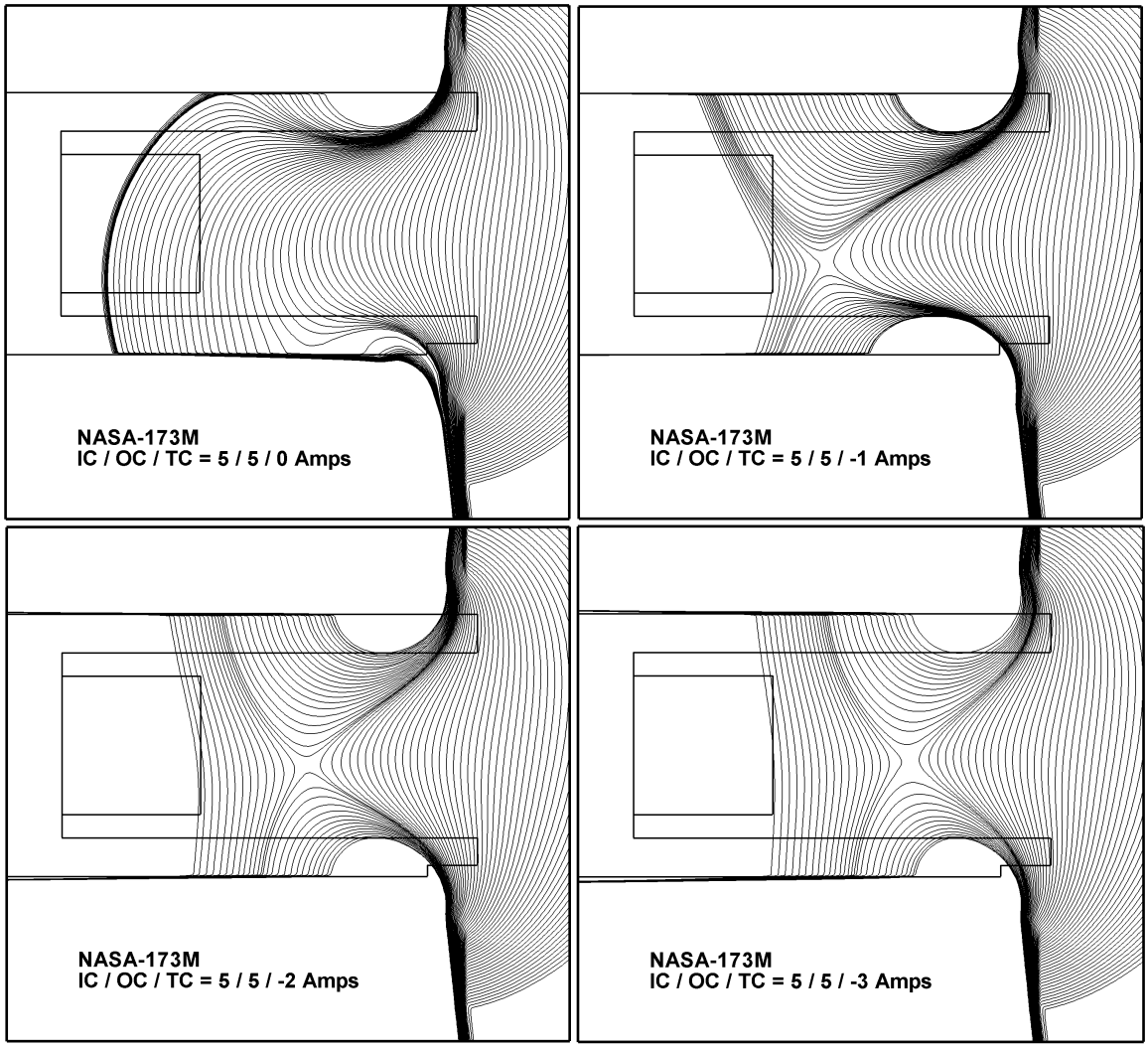

Figure 18 - Magnetic field line topography at several trim coil (TC) currents and constant inner (IC) and outer coil (OC) currents of 5 A.

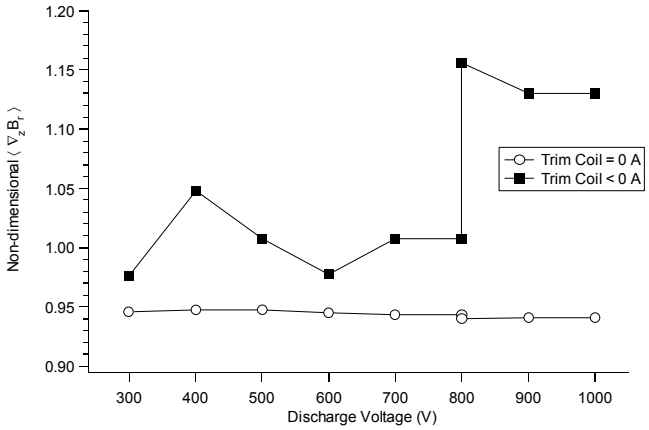

Figure 19 – Non-dimensional gradient of the magnetic field vs. discharge voltage.

Appendix

Table 1- NASA-173M performance data at 300-600 V, 5 mg/s.

Vd (V)	Id (A)	Iic (A)	Ioc (A)	Itc (A)	Thrust (mN)	Anode Isp (s)	Anode Eff	Vcg (V)	Anode (mg/s)	Cathode (mg/s)
300.1	4.18	2.00	1.50	0.00	75.0	1530	0.449	-12.5	5.00	0.54
300.5	4.20	2.00	1.50	0.00	75.3	1542	0.452	-13.5	4.98	0.52
300.5	4.18	2.00	1.50	-0.12	75.9	1554	0.461	-13.6	4.98	0.52
300.6	4.15	2.00	1.50	-0.22	75.6	1548	0.461	-13.5	4.98	0.52
300.6	4.13	2.00	1.50	-0.30	75.2	1539	0.457	-13.2	4.98	0.52
300.1	4.17	2.00	1.49	-0.44	74.1	1517	0.441	-12.3	4.98	1.02
300.0	4.20	2.00	1.49	-0.53	74.2	1519	0.439	-12.1	4.98	1.02
299.9	4.33	2.00	1.49	-1.01	71.1	1454	0.391	-11.4	4.98	1.02
400.0	4.18	1.99	1.50	0.00	90.3	1841	0.487	-12.9	5.00	0.54
400.4	4.20	2.06	2.04	-0.09	91.0	1862	0.494	-13.3	4.98	0.52
400.1	4.26	2.06	2.04	-0.27	91.9	1880	0.497	-12.7	4.98	1.02
400.4	4.37	2.06	2.04	-0.44	93.6	1917	0.503	-12.8	4.98	1.02
400.1	4.37	2.06	2.04	-0.50	92.8	1900	0.495	-12.8	4.98	1.02
400.3	4.44	2.06	2.04	-0.60	92.4	1891	0.482	-12.6	4.98	1.02
400.2	4.49	2.06	2.04	-0.75	89.1	1824	0.443	-12.5	4.98	1.02
500.4	4.52	2.00	2.00	0.00	105.5	2160	0.495	-12.5	4.98	1.02
500.4	4.51	2.00	1.99	0.00	106.1	2171	0.500	-12.4	4.98	1.02
500.3	4.46	2.00	1.99	-0.09	106.2	2175	0.508	-12.7	4.98	1.02
500.4	4.51	2.00	1.99	-0.22	107.1	2193	0.510	-12.3	4.98	1.02
500.2	4.50	2.00	1.99	-0.27	107.1	2192	0.512	-12.4	4.98	1.02
500.1	4.59	2.00	1.99	-0.40	107.2	2194	0.502	-12.2	4.98	1.02
500.1	4.68	2.00	1.99	-0.53	106.6	2182	0.487	-11.9	4.98	1.02
500.1	4.68	2.00	1.99	-1.01	102.7	2102	0.452	-11.7	4.98	1.02
600.4	4.63	3.03	2.99	0.00	119.0	2436	0.511	-14.0	4.98	0.52
600.5	4.57	3.03	2.99	0.00	118.7	2429	0.515	-13.9	4.98	0.52
600.3	4.55	3.03	3.00	-0.12	118.0	2416	0.512	-14.0	4.98	0.52
600.2	4.64	3.03	2.99	-0.22	120.0	2455	0.519	-14.1	4.98	0.52
600.0	4.75	3.03	2.99	-0.37	120.5	2467	0.511	-13.7	4.98	0.52
600.1	4.83	3.03	2.99	-0.50	120.1	2459	0.500	-13.4	4.98	0.52
600.0	4.94	3.03	2.99	-1.03	118.4	2424	0.475	-12.9	4.98	0.52
600.0	4.93	3.03	2.99	-2.03	114.2	2337	0.443	-12.7	4.98	0.52
600.4	4.75	3.03	2.99	-3.07	107.7	2204	0.408	-12.5	4.98	0.52

Table 2 - NASA-173M performance data at 700-1000 V, 5 mg/s.

Vd (V)	Id (A)	Iic (A)	Ioc (A)	Itc (A)	Thrust (mN)	Anode Isp (s)	Anode Eff	Vcg (V)	Anode (mg/s)	Cathode (mg/s)
700.3	4.77	3.52	3.47	0.00	128.2	2625	0.494	-13.6	4.98	0.52
700.3	4.77	3.52	3.47	0.00	128.4	2628	0.496	-13.5	4.98	0.52
700.4	4.72	3.52	3.48	0.00	128.1	2622	0.499	-13.9	4.98	0.52
700.3	4.76	3.52	3.47	-0.27	129.0	2641	0.501	-13.7	4.98	0.52
700.5	4.70	3.52	3.47	-0.27	128.4	2627	0.502	-14.0	4.98	0.52
700.6	4.66	3.52	3.47	-0.50	128.0	2620	0.503	-14.0	4.98	0.52
700.4	4.74	3.52	3.47	-0.52	129.2	2645	0.505	-13.7	4.98	0.52
700.4	4.73	3.52	3.47	-0.75	128.7	2634	0.502	-13.7	4.98	0.52
700.5	4.74	3.52	3.47	-0.75	128.6	2633	0.501	-13.8	4.98	0.52
700.2	4.91	3.51	3.47	-1.03	129.7	2655	0.491	-13.2	4.98	0.52
700.0	5.02	3.51	3.47	-1.23	129.2	2646	0.477	-12.8	4.98	0.52
700.0	5.03	3.51	3.47	-1.50	128.1	2623	0.468	-12.6	4.98	0.52
799.5	4.75	3.50	3.50	0.00	135.0	2752	0.480	-12.3	5.00	0.54
800.5	4.87	3.52	3.48	0.00	136.9	2802	0.483	-12.9	4.98	0.52
800.6	4.83	3.51	3.49	0.00	136.7	2797	0.485	-13.1	4.98	0.52
800.5	4.86	3.52	3.48	-0.27	137.8	2820	0.489	-12.9	4.98	0.52
800.6	4.81	3.51	3.48	-0.27	137.0	2804	0.489	-13.1	4.98	0.52
800.7	4.80	3.51	3.48	-0.50	137.2	2809	0.492	-13.2	4.98	0.52
800.6	4.85	3.52	3.48	-0.50	138.3	2831	0.495	-13.0	4.98	0.52
800.7	4.85	3.51	3.48	-0.75	138.0	2825	0.492	-13.0	4.98	0.52
800.7	4.81	3.51	3.48	-0.75	137.0	2805	0.490	-13.2	4.98	0.52
800.6	4.95	3.51	3.48	-1.00	138.3	2832	0.485	-12.8	4.98	0.52
800.2	5.20	3.51	3.48	-1.50	138.5	2834	0.463	-11.9	4.98	0.52
800.5	4.83	4.54	4.52	0.00	135.2	2768	0.475	-13.7	4.98	0.52
800.5	4.85	4.54	4.52	-1.01	138.3	2832	0.495	-13.8	4.98	0.52
800.4	4.94	4.54	4.52	-2.05	140.3	2871	0.500	-13.6	4.98	0.52
800.2	5.12	4.54	4.52	-3.05	139.3	2851	0.475	-13.0	4.98	0.52
900.4	5.08	5.03	4.99	0.00	146.8	2994	0.471	-10.8	5.00	1.02
900.5	5.07	5.03	4.99	-1.05	149.3	3044	0.488	-10.9	5.00	1.02
900.6	5.10	5.03	4.99	-2.06	152.0	3099	0.503	-10.8	5.00	1.02
900.4	5.47	5.02	4.99	-3.03	153.4	3127	0.478	-10.0	5.00	1.02
900.2	5.51	5.03	4.99	-3.03	153.9	3137	0.477	-9.8	5.00	1.02
1003.2	5.20	4.98	4.97	0.00	154.9	3159	0.460	-10.0	5.00	1.02
1003.4	5.19	4.98	4.97	-1.01	159.8	3258	0.490	-10.2	5.00	1.02
1003.5	5.18	4.98	4.97	-1.53	160.3	3269	0.494	-9.9	5.00	1.02
1003.7	5.26	4.98	4.97	-2.03	164.9	3362	0.515	-10.2	5.00	1.02
1000.5	5.67	5.02	4.99	-3.03	162.1	3305	0.463	-9.3	5.00	1.02
1003.4	5.74	5.01	4.98	-3.03	163.2	3328	0.463	-9.2	5.00	1.02